Vol. 41, No. 3 (2019) 394-400, DOI: 10.24874/ti.2019.41.03.09

Tribology in Industry

www.tribology.rs

RESEARCH

Corrosion Rate and Wear Mechanisms Comparison for Aisi 410 Stainles Steel Exposed to Pure Corrosion and Abrasion-corrosion in a Simulated Marine Environment

G.A. Rodríguez-Bravo[a], M. Vite-Torres[a], J.G. Godínez-Salcedo[b]

[a] *Instituto Politécnico Nacional, SEPI ESIME Zacatenco, Ciudad de México, México,*
[b] *Instituto Politécnico Nacional, SEPI ESIQIE Zacatenco, Ciudad de México, México.*

Keywords:

Tribocorrosion
Corrosion rate
Seawater
Abrasion-corrosion
AISI 410

Corresponding author:

Manuel Vite-Torres
Instituto Politécnico Nacional,
SEPI ESIME Zacatenco, Ciudad de México, México.
E-mail: drmanuelvite9@hotmail.com

A B S T R A C T

Due to its diversity of applications in mechanical components such as; pumps, valves and turbine parts, AISI 410 stainless steel is exposed to combined conditions of wear and corrosion. Although several works have been carried out to evaluate some properties of this steel, there is not enough information about the changes in its corrosion rate when the work conditions change from pure corrosion to abrasion-corrosion in a marine environment, so it is necessary to delve into an analysis from the tribocorrosion perspective, since it is still been a phenomenon not completely understood. This work presents results of AISI 410 corrosion rate analysis, carried out in a novel test rig based on ASTM G-105 wet sand apparatus but adapted with an electrochemical corrosion cell to contain the corrosive medium. Two electrochemical techniques were used: polarization resistance (Rp), and anodic potentiodynamic polarization. Substitute ocean water (aqueous medium), and silica sand (abrasive particles) were used to recreate the medium. SEM analysis was performed after each test to determine wear mechanisms. Material does not present a good corrosion resistance under pure corrosion condition contrary to abrasion-corrosion. Polarization curves do not show a passivation zone of the material when it is submerged in medium.

1. INTRODUCTION

AISI 410 stainles steel (Ss) is the more available of the martensitic Ss, also is cheaper than almost all of the others. Availability makes AISI 410 Ss to be commonly used in diverse applications that requires good mechanical properties and also corrosion resistance. Several components are fabricated with this material and used in industries like hydrocarbon extraction, energy generation, chemical plants, engine/turbine fabrication, and also the marine industries [1-2]. Sometimes the diversity of applications of this

material make it to be exposed to conditions of combined forms of degradation like the case of components for the marine industry where the aggressiveness of seawater is combined with the abrasive effect of sand particles generating tribocorrosion. This phenomenon is defined as the action of electrochemical degradation (corrosion) and mechanical wear happening simultaneously in an aggressive medium. Rarely the tribocorrosion effect is just the sum of mechanical wear plus corrosive wear, but generally it is higher (synergistic interaction) or lower (antagonistic interaction) [3]. In literature, two main forms of tribocorrosion can be found: abrasion-corrosion and erosion-corrosion. These forms of tribocorrosion can be generated by different mechanisms like: fretting, sliding, rolling, or impingement. Each mechanism can have its own variations [4].

Martensitic Ss have been evaluated in different conditions like pure corrosion, erosion, and erosion-corrosion [5-6]. Abrasion-corrosion has been evaluated in this kind of steels using a pin on disk tribometer (two body unidirectional sliding to generate mechanical wear in a corrosive medium) together with a potentiostat to perform electrochemical tests [7-8]. Most commonly used electrochemical techniques to evaluate corrosion are: Open circuit potential, TAFEL plot, polarization resistance, and anodic potentiodynamic polarization [9].

Even though AISI 410 have some applications in components used in marine environments, there are not enough information available about its performance when is exposed to abrasion-corrosion in those conditions.

In this work is presented an evaluation of the tribocorrosion properties of AISI 410 Ss in pure corrosion and abrasion-corrosion condition, simulating a marine environment. Evaluation consists in compare corrosion rates in both work conditions. A novel test rig (based on the ASTM G-105 wet sand rubber apparatus) that recreates a three-body unidirectional sliding situation was used together with a potentiostat to perform simultaneously the mechanical damage, accelerated corrosion, and corrosion rate measurements. Test rig was designed and developed by the IPN ESIME Zacatenco tribology group [10].

2. EQUIPMENT AND MATERIALS

2.1 Abrasion-corrosion tester details and experimental arrangement

Test rig is addapted with an electrochemical corrosion cell to perform the neccesary tests to evaluate corrosion [11]. The sampler holder is also adapted to allow te linking cables to connect the electrodes to the potentiostat while it works like a load applier as its showed in Fig. 1.

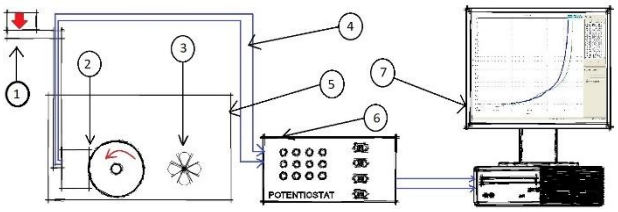

Fig. 1. Experimental arrangement: 1. Load applier; 2. Sample holder-rubber wheel interface; 3. Aqueous medium mixer; 4. Electrodes cables; 5. Electrochemical corrosion cell; 6. Potentiostat; 7. Data processing software.

There are some works in literature that have used the same contact configuration and similar test rigs. This configuration consist in a metallic sample (work electrode) having contact against a sliding counter body submerged in an aggressive medium with the presence of suspended abrasive particles (abrasive slurry) [12-13]. This machine adaptation allows the sample/electrode holder to work also as load applier trough a lever arm system.

As can be seen in Fig. 2, the counter body is a rubber wheel that has a softer surface than the metallic sample so the contact does not produce any damage in the material; the only function of the counter body is to oppose the load applied and move the silica sand particles in one direction to evaluate their effect in the corrosion rate.

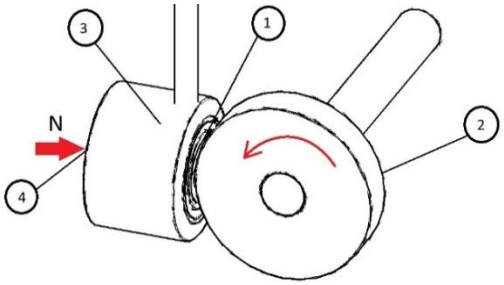

Fig. 2. Schematic representation of contact configuration: 1. Work electrode; 2. Rubber wheel; 3. Sample holder; 4. Load direction.

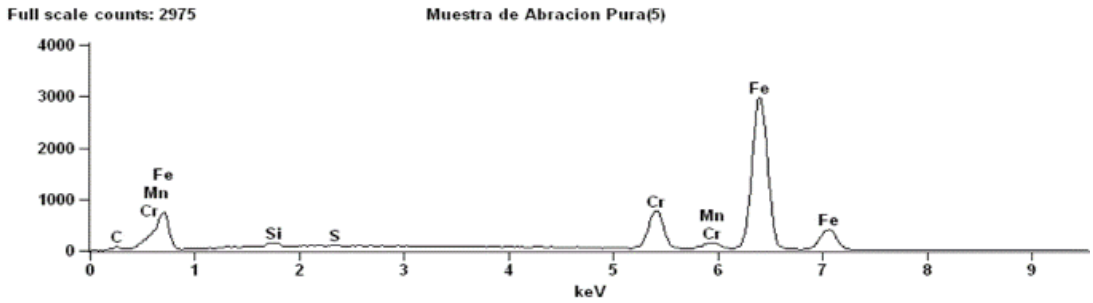

Fig. 3. EDS analysis of AISI 410 stainless steel.

2.2 Samples

AISI 410 Ss samples were obtained from a round commercial rod, presenting a Vickers hardness of 210 during the mechanical properties characterization. Chemical composition was determined by electron diffraction spectrometry (EDS) and results can be seen in Fig. 3. Results were compared with datasheet to confirm that material was within range as can be seen in Tables 1 and 2.

Sample´s geometry was determined to have a flat circular face with an approximate area of 1 cm^2; to simplify all the calculations and have a good control of experimentation parameters. . Density of material is 7.75 g/cm^3.

Table 1. Chemical composition of AISI 410 stainless steel according to data sheet [14].

Element	Maximun Concentration (%)
C	0.08 – 0.15
Mn	1.0
S	.030
P	.040
Si	1.0
Cr	11.5 – 13.5
Ni	0.75

Table 2. Element concentration according to EDS analysis of samples.

Element Line	*Weight %*	*Atom %*
Si K	0.49	0.96
S K	0.03	0.12
Cr K	12.10	12.81
Mn K	0.39	0.39
Fe K	86.95	85.71
Total	100.00	100.00

Instead of the commonly used Sturated Calomel (KCl), and graffite electrodes; two metallic rings made of the same working material (AISI 410 Ss) were asigned as reference electrode and counter electrode [15].

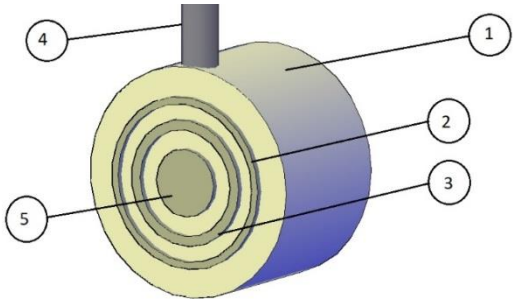

Fig. 4. Schematic representation of sample and electrodes in polyester resine: 1. Polyester resine; 2. Counter electrode; 3. Referene electrode; 4. Cables exit; 5. Working electrode.

Figure 4 shows the sample configuration that allows to have a central AISI 410 Ss working electrode surrounded by the other two electrodes, both mounted in polyester resine [16].

2.3 Abrasive particles

Silica sand (SiO_2) from tribology group stock with: sharped edges, average size of 171.5 μm, and hardness of 789.5 Vickers; was used to represent accurately the particles presents in a marine work environment. Electron microscopy (SEM) to determine morphology is showed in Fig. 5 [17].

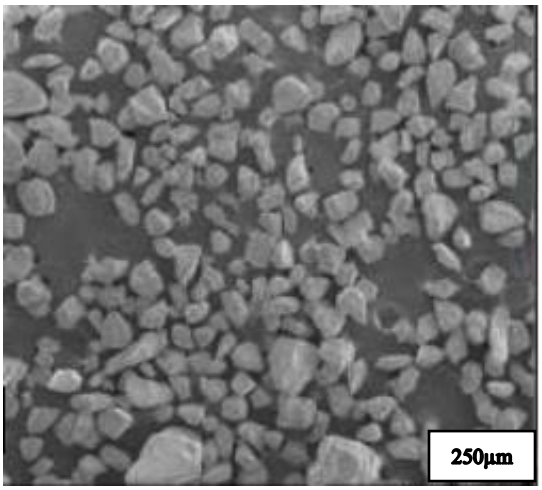

Fig. 5. SEM micrographs of silica sand particles.

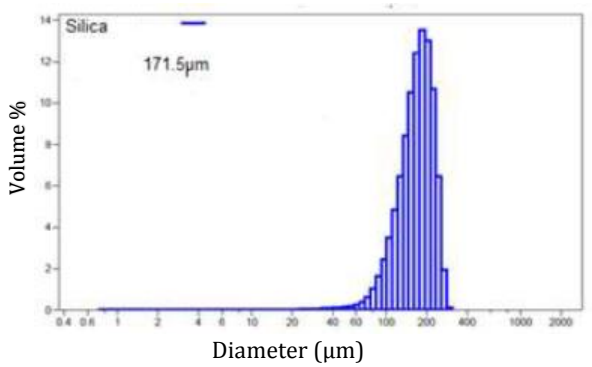

Fig. 6. Sand particles size distribution.

Laser distribution analysis was performed to calculate the average particle size; results are showed in Fig. 6.

2.4 Corrosive medium

Substitute ocean water was used as corrosive medium to simulate marine conditions. It is a solution with content of inorganic salts in representative proportions and concentrations of seawater. Its preparation is normalized by ASTM International [18]. Table 3 shows concentration of chemical compounds used to prepare substitute ocean water.

Table 3. Chemical compounds in substitute ocean water according to norm ASTM D1141-98(2013).

Compound	Concentration (gr/l)
NaCl	24.53
$MgCl_2$	5.20
Na_2SO_4	4.09
$CaCl_2$	1.16
KCl	0.695
$NaHCO_3$	0.201
KBr	0.101
H_3BO_3	0.027
$SrCl_2$	0.025
NaF	0.003

Aqueous medium was stabilized in an 8.2 pH

3. METHODS

Techniques used in this experimental procedure on two AISI 410 Ss samples were: Open circuit measurement (Ocm) to determine corrosion potential (E_{Corr}), Polarization resistance (Rp) to calculate corrosion rate, and potentiodynamic anodic polarization (Pap) to analyse and compare the characteristic sample polarization plot generated. Each technique was practiced in pure corrosion and abrasion-corrosion conditions. To recreate the marine work conditions in a controlled way, each test was performed in 1 L of substitute ocean water. Table 4 shows the parameter values used to reproduce both of test conditions. Parameters controlled were: Counter body load (load, N), Abrasive particle concentration (Apc, gr), and sliding velocity (Vs, m/min).

Table 4. Test parameters.

Sample ID	Performed Test	Tests condition	Parameters value	
AISI410-1	Ocm	Pure corrosion	No particles or sliding	
	Rp			
	Pap			
AISI410-2	Ocm	Abrasion - corrosion	150 gr	Apc
	Rp		2.5 N	Load
	Pap		30 m/min	Vs

Corrosion rate (V_{corr}) is expressed in mill-inches per year (mpy). For this work, corrosion rate was calculated using Rp technique that consist in an electric potential scanning trough a potential range very close to the E_{Corr} (±20 mV). The resulting current of the scanning is measured and plotted against the potential then related with V_{corr} as can be seen in equation 1.

$$\text{Vcorr(mpy)} = \frac{0.13\ \text{Icorr (E.W.)}}{d} \quad (1)$$

Were "I_{corr}" is the measured corrosion current density ($\mu A/cm^2$), "E.W." is the equivalent weight of the corroding specie, and "d" is the density of the material (gr/cm^3). Each sample is tested five time with "Rp" to use an average of the calculated corrosion rates. To generate the polarization plot is used the "Pap" technique. For this test the potential sweep was from was -200 mV to +1600 mV at a step velocity of .166 mv/S. This plot is important to obtain information like: Potential region in which the material remains passive, identify potential regions of the material and calculate corrosion rate in a certain one [19]. Once that both sample has been tested, these are analysed using the electron microscope to identify mechanisms presents in the wear process.

4. RESULTS

The Ocm resulting plot can be observed in Fig. 7. "Ocm" in Abrasion-corrosion condition got values between -0.359 and -0.059 mV; pure corrosion between -0.357 and -0.441 mV. Also

Instability was observed while in pure corrosion the values are stables. This difference is an indicator of reactivity decrease in the sample-medium interface due to the presence of abrasive slurry in the sample surface. Corrosion rate calculated by "Rp" in pure corrosion was 1.087 mpy while in abrasion-corrosion was .144 mpy. This is a decrease of 87 % in corrosion. Decreasing of corrosion rate value confirm the difficult to made the electron exchange between species when the mechanical wear has occurred and can be attributed to a saturation of sand particles on the contact surface. Difference in corrosion rate can be observed in Fig. 8.

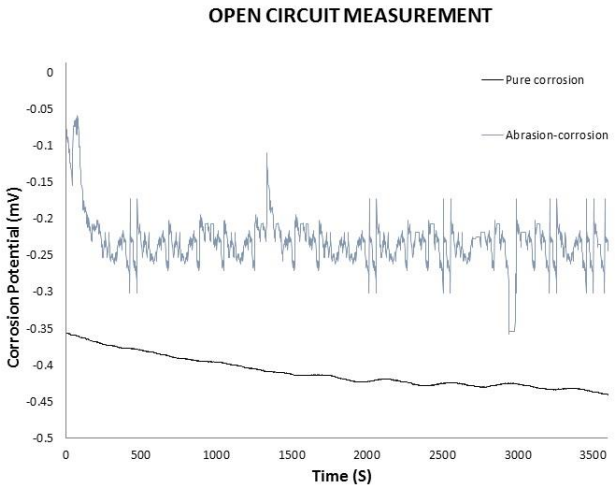

Fig. 7. Open circuit plot of AISI 410 stainless steel in pure corrosion and abrasion-corrosion.

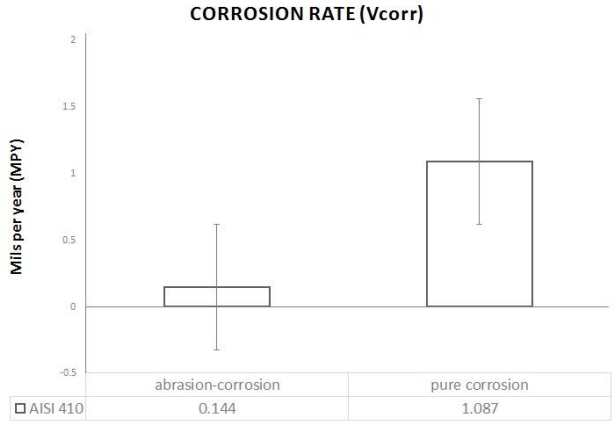

Fig. 8. Corrosion rate comparison.

Polarization curve plots are graphic representations of material electrochemical response in medium obtained by applying "Pap". A comparison of polarization curves of AISI 410 Ss in both conditions is showed in Fig. 9.

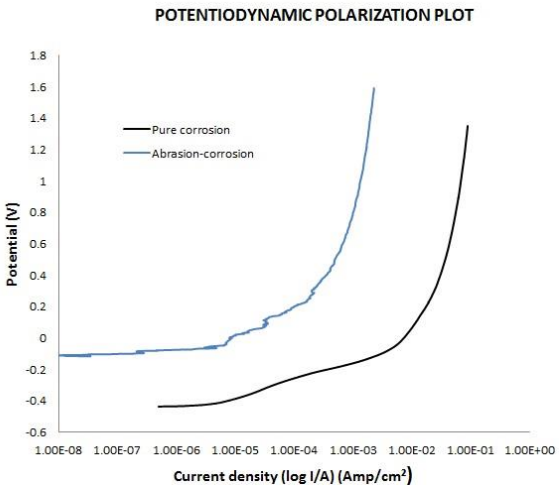

Fig. 9. Polarization curves comparison.

A reduction in current density can be seen in the abrasion-corrosion curve plot; this confirm the decrease in corrosion rate when the sand particles were present in the sample surface. None of the curves showed a real passivation zone of the material which is an indicator of the bad performance of this steel in a medium like substitute ocean water. The absence of a passivation zone can be attributed to the presence of chloride ions; the reduction of passive oxide layer in mediums with high content of chloride ions has been reported in literature [20].

Figure 10 shows material detachment from the sample surface after the pure corrosion "Pap" test. In figure 11, a close up of this detachment shows traces of intergranular corrosion. This can be caused by sensitization of the oxide layer in grain boundaries, phenomenon that have been correlated with pitting corrosion of martensitic stainless steels in previous studies [21].

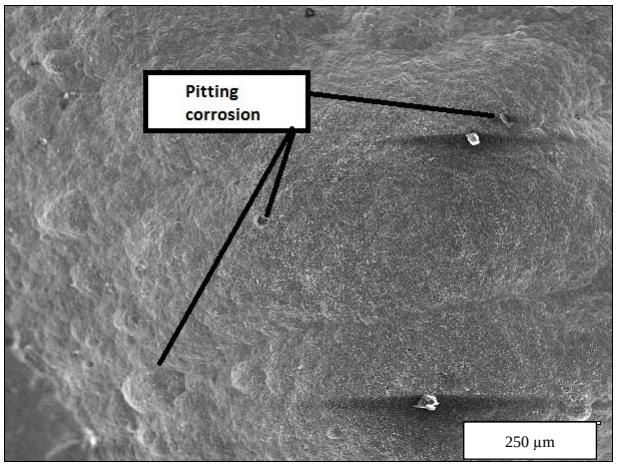

Fig. 10. SEM view of material after "Pap".

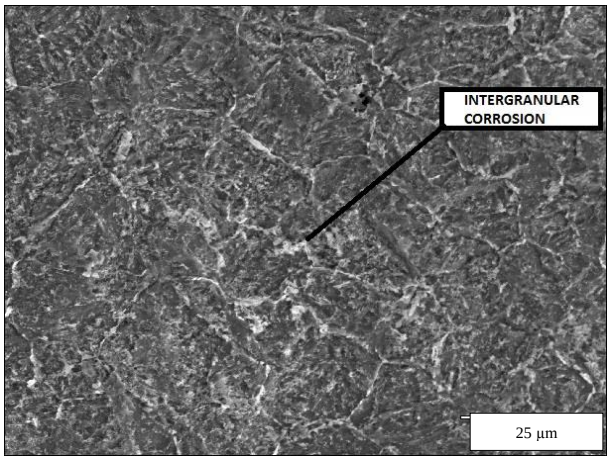

Fig. 11. SEM view of intergranular corrosion after pure corrosion test.

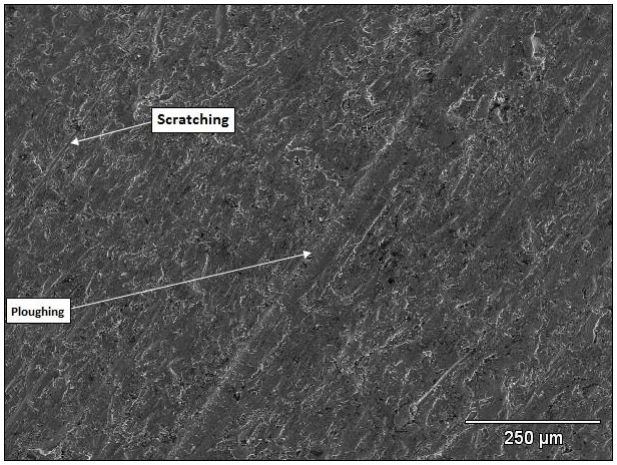

Fig. 12. Electron microscope image of sample surface after abrasion-corrosion.

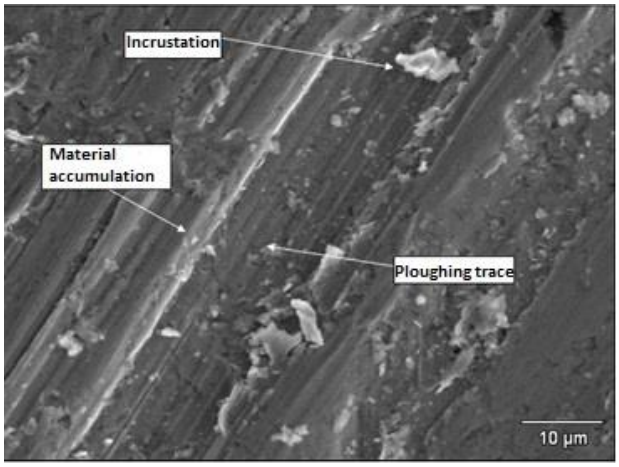

Fig. 13. Close up of ploughing trace.

Wear mechanisms found in abrasion-corrosion are showed in Figs. 12 and 13. Only traces of mechanical wear were observed. Ploughing and scratching are the main forms of wear presents in the sample surface, generating material accumulation in the edges of the scars, this is characteristic of abrasive wear. Also some incrustations of abrasive particles were found.

5. CONCLUSIONS

Results indicate that:

- The reduction of visible signs of corrosion confirms the decreasing of corrosion rate in abrasion-corrosion condition indicated by the electrochemical tests.
- There is not a good corrosion resistance to marine environment in AISI 410 Ss; this can be attributed to a reduction in the passive oxide film caused by chloride ions.
- Sand particles on the sample surface inhibit the corrosive effects of medium. This corresponds to an antagonistic effect of the abrasion-corrosion phenomenon.
- Mechanical wear predominates over corrosion.

Acknowledgment

Thanks to CONACYT and IPN-COFAA for the economic support. Also to IPN SEPI ESIME Zacatenco tribology group, and to the corrosion laboratory of IPN ESIQIE Zacatenco for the support to carry out the experiments necessaries to complete this work.

REFERENCES

[1] R.T. Loto, *Study of the corrosion behaviour of S32101 duplex and 410 martensitic stainless steel for application in oil refinery distillation systems,* Journal of Materials Research and Technology, vol. 6, iss. 3, pp. 203–212, 2017, doi: 10.1016/j.jmrt.2016.11.001

[2] P.D. Krell, S. Li, H. Cong, *Synergistic effect of temperature and HCl concentration on the degradation of AISI 410 stainless steel,* Corrosion Science, vol. 122, pp. 41–52, 2017, doi: 10.1016/j.corsci.2017.03.027

[3] S. Mischler, A.I. Munoz, *Tribocorrosion,* Reference Module in Chemestry Molecular Sciences and Chemical Engineering – Encyclopedia of Interfacial Chemistry, pp. 504–514, 2017, doi: 10.1016/B978-0-12-409547-2.13424-9

[4] A.I. Muoz, N. Espallargas, 5-*Tribocorrosion mechanisms in sliding contacts,* Tribocorrosion of

Passive Metals and Coatings, pp. 118–152, 2017, doi: 10.1533/9780857093738.1.118

[5] L.A. Espitia, L. Varela, C.E. Pinedo, A.P. Tschiptschin, *Cavitation erosion resistance of low temperature plasma nitrided martensitic stainless steel,* Wear, vol. 301, iss. 1–2, pp. 449–456, 2013, doi: 10.1016/j.wear.2012.12.029

[6] D. López, A.P. Tschiptschin, N.A. Falleiros, *Sinergismo Erosión-Corrosión En Un Acero Inoxidable Martensítico Aisi 410: Erosion-Corrosion Synergism of an Aisi 410 Martensitic Stainless Steel*, Dyna, vol. 76, no. 159, pp. 53–60, 2009.

[7] A. Dalmau, W. Rmili, C. Richard, A. Igual–Muñoz, *Tribocorrosion behavior of new martensitic stainless steels in sodium chloride solution,* Wear, vol. 368–369, pp. 146–155, 2016, doi: 10.1016/j.wear.2016.09.002

[8] A. Dalmau, C. Richard, A. Igual – Muñoz, *Degradation mechanisms in martensitic stainless steels: Wear, corrosion and tribocorrosion appraisal,* Tribology International, vol. 121, pp. 167–179, 2018, doi: 10.1016/j.triboint.2018.01.036

[9] D. Landolt, S. Mischler, M. Stemp, *Electrochemical methods in tribocorrosion: A critical appraisal,* Electrochimica Acta, vol. 46, iss. 24–25, pp. 3913–3929, 2001, doi: 10.1016/S0013-4686(01)00679-X

[10] G.A. Rodríguez-Bravo, *Estudio del comportamiento del acero AISI 410 sometido al fenómeno de abrasión húmeda-Corrosión,* Master degree thesis, SEPI ESIME Zacatenco, Instituto Politécnico Nacional, ciudad de México, México, 2017.

[11] ASTM G105-16, *Standard Test Method for Conducting Wet Sand/Rubber Wheel Abrasion Tests*, 2016.

[12] G.B. Stachowiak, M. Salasi, W.D.A. Rickard, G.W. Stachowiak, *The effects of particle angularity on low-stress three-body abrasion-corrosion of 316L stainless steel,* Corrosion Science, vol. 111, pp. 690–702, 2016, doi: 10.1016/j.corsci.2016.06.008

[13] M.B. Santos, W.S. Labiapari, M.A.N. Ardila, W.M. Da Silva, J.D.B. De Mello, *Abrasion-corrosion: New insights from force measurements,* Wear, vol. 332–333, pp. 1206–1214, 2015, doi: 10.1016/j.wear.2015.01.002

[14] Specification Sheet: Alloy 410, Available at: https://www.sandmeyersteel.com/images/410-Spec-Sheet.pdf

[15] Princeton Applied Research Center, *Electrochemistry and Corrosion: Overview and Techniques,* TN, USA, 2017.

[16] C. Sedano, *Estudio experimental del comportamiento de los aceros para ductos sometidos a erosión-corrosión,* PhD thesis, SEPI ESIME Zacatenco, Instituto Politécnico Nacional, ciudad de México, México, 2017.

[17] A.H. Mayen, *Estudio del coeficiente de fricción en asfalto con presencia de hielo y arena empleando el pendulo deslizante,* Masters degree thesis, SEPI ESIME Zacatenco, Instituto Politécnico Nacional, Ciudad de México, México, 2017.

[18] ASTM D1141-98(2013), *Standard Practice for the Preparation of Substitute Ocean Water*, 2013.

[19] B.N. Popov, *Chapter 5 - Basics of Corrosion Measurements,* Corrosion Engineering, pp. 181–237, 2015, doi: 10.1016/b978-0-444-62722-3.00005-7

[20] A. Fattah-alhosseini, M.H. Fahim, E. Nikomanzari, *The Effect of Chloride Ions Concentration on the Electrochemical Behavior of AISI 410 Stainless Steels in Simulated Concrete Pore Solution,* International journal of ISSI, vol. 11, no. 1, pp. 35–40, 2014.

[21] I. Taji, M.H. Moayed, M. Mirjalili, *Correlation between sensitisation and pitting corrosion of AISI 403 martensitic stainless steel,* Corrosion Science, vol. 92, pp. 301–308, 2015, doi: 10.1016/j.corsci.2014.12.009